

Original Paper

Investigation of the Inhibitory Effects of the Benzodiazepine Derivative, 5-BDBD on P2X₄ Purinergic Receptors by two Complementary Methods

Bernadett Balázs^a Tamás Dankó^a Gergely Kovács^{b,c} László Köles^d Matthias A. Hediger^{b,c} Ákos Zsembery^a

^aInstitute of Human Physiology and Clinical Experimental Research, Semmelweis University, Budapest;

^bInstitute of Biochemistry and Molecular Medicine, University of Bern; ^cSwiss National Centre of Competence in Research, NCCR TransCure, University of Bern; ^dDepartment of Pharmacology and Pharmacotherapy, Semmelweis University, Budapest

Key Words

Calcium influx • Electrophysiology • ATP • 5-BDBD • P2X receptors

Abstract

Background/Aims: ATP-gated P2X₄ purinergic receptors (P2X₄Rs) are cation channels with important roles in diverse cell types. To date, lack of specific inhibitors has hampered investigations on P2X₄Rs. Recently, the benzodiazepine derivative, 5-BDBD has been proposed to selectively inhibit P2X₄Rs. However, limited evidences are currently available on its inhibitory properties. Thus, we aimed to characterize the inhibitory effects of 5-BDBD on recombinant human P2X₄Rs. **Methods:** We investigated ATP-induced intracellular Ca²⁺ signals and whole cell ion currents in HEK 293 cells that were either transiently or stably transfected with hP2X₄Rs. **Results:** Our data show that ATP (< 1 μM) stimulates P2X₄R-mediated Ca²⁺ influx while endogenously expressed P2Y receptors are not activated to any significant extent. Both 5-BDBD and TNP-ATP inhibit ATP-induced Ca²⁺ signals and inward ion currents in a concentration-dependent manner. Application of two different concentrations of 5-BDBD causes a rightward shift in ATP dose-response curve. Since the magnitude of maximal stimulation does not change, these data suggest that 5-BDBD may competitively inhibit the P2X₄Rs. **Conclusions:** Our results demonstrate that application of submicromolar ATP concentrations allows reliable assessment of recombinant P2XR functions in HEK 293 cells. Furthermore, 5-BDBD and TNP-ATP have similar inhibitory potencies on the P2X₄Rs although their mechanisms of actions are different.

Copyright © 2013 S. Karger AG, Basel

Introduction

Extracellular ATP and its breakdown products regulate a number of cellular functions by stimulating purinergic receptors [1]. In the last two decades 19 different purinergic receptors have been identified including four adenosine-activated P1 receptors, seven ATP-gated P2X receptor (P2XR) channels and eight metabotropic P2Y receptors which can be stimulated by adenosine and uridine tri- and diphosphates [2].

The seven P2X receptor subunits (P2X₁₋₇) are widely distributed in both excitable and non-excitable cells providing cation permeable pathways (mainly for Ca²⁺ and Na⁺) through the plasma membrane. Previous studies revealed that these subunits might assemble as either homo- or heterotrimeric receptors [2]. Importantly, heteromerization can change functional and pharmacological properties of the P2XRs [2]. P2XRs are involved in presynaptic and postsynaptic actions of ATP [3-5] including taste sensation [6], hearing [7] and chemoreception [8]. P2XRs are also necessary for proper function of immune system [9]. In cardiovascular, respiratory, genitourinary and gastrointestinal systems several P2X receptor subunits seem to play pivotal role in both endothelial and epithelial cell functions [10]. Using pharmacological approaches and knockout animals, it has also become evident that P2XRs are involved in a broad range of pathophysiological processes such as chronic and inflammatory pain [11-15] arthritis [16] male infertility [17] and hypertension [18, 19].

A role for P2X₄ receptors has been proposed in neuropathic pain [15], endothelial NO production [18], regulation of airway ciliary epithelia [20] and chloride secretion of respiratory [21, 22] and biliary epithelia [23]. However, validation of P2X₄R involvement has been often hampered by the lack of specific inhibitors. In fact, P2X₄ receptors are insensitive to the nonselective inhibitors, such as suramin and PPADS [24]. TNP-ATP has been found as a putative antagonist of P2X₄ receptors. However, it blocks other P2X subtypes as well, such as P2X₁, P2X₂ and P2X₃ [25]. Furthermore, TNP-ATP has been shown to be a weak blocker of P2X₄ receptors (IC₅₀ = 15 μM for 10 μM ATP stimulation) compared to its inhibitory potency at P2X₁ and P2X₃ receptors [26].

The benzodiazepine derivative, 5-(3-bromophenyl)-1,3-dihydro-2H-benzofuro[3,2-e]-1,4-diazepin-2-one (5-BDBD), has been recently shown to selectively inhibit P2X₄ receptors (IC₅₀ ~ 0.5 μM) [27]. Nonetheless, these results are described in a patent and details of the experimental procedure are not available. So far, limited experience has been available with 5-BDBD and there is no consensus about its pharmacologically relevant concentration range. In some studies low micromolar (5-10 μM) concentrations were used [28, 29] whereas others applied significantly higher doses of 5-BDBD (30-100 μM) [30, 31].

In the present study, we investigated ATP-induced cytosolic Ca²⁺ signals and inward ion currents in HEK 293 cells transfected either transiently or stably with hP2X₄ receptors. We characterized P2X₄ receptor-mediated whole cell ion currents and identified P2YR- and P2XR-dependent calcium signals using electrophysiological and fluorescence ion measurement techniques, respectively. Despite endogenous expression of P2YRs we were able to discern P2XR-dependent Ca²⁺ signals stimulating the cells with submicromolar concentrations of ATP. We also assessed the inhibitory effects of 5-BDBD and TNP-ATP on both intracellular Ca²⁺ signals and inward ion currents. Our data suggest that 5-BDBD and TNP-ATP have similar inhibitory potencies on P2X₄Rs. Furthermore, we show that 5-BDBD functions as a competitive antagonist of hP2X₄Rs.

Materials and Methods

Materials

Cell culture medium, fetal bovine serum, cell culture supplements and antibiotics were purchased from Cserterx Inc. (Budapest, Hungary). TurboFect™ *in vitro* Transfection Reagent was purchased from Biocenter (Szeged, Hungary). Lipofectamine 2000 was obtained from Invitrogen (Life Technologies Europe B.V, Zug, Switzerland). Fluo-3/AM was purchased from Invitrogen Inc. (Carlsbad, CA). 5-BDBD was obtained

from Tocris Inc. (Minneapolis, USA). Calcium-5 was purchased from Molecular Devices (Molecular Devices LLC, Sunnyvale, CA, USA). Ivermectin (IVM) was obtained from Merck AG (Merck, Zug, Switzerland). All other chemicals were purchased from Sigma-Chemical (St. Louis, MO).

DNA Construct

The human P2X₄R (imaGenes GmbH, Berlin, Germany) was amplified from human cDNA with the following primer pair: 5'-TAT AAG ATC TCG CGG CCA TGG CGG GC-3',

5'-TAT AGA ATT CCC TGG TCC AGC TCA CTA GCA AGA CCC TGC-3'

The amplified product was subcloned into the pmCherry-N1 (Clontech Laboratories Inc.) vector by using BglII and EcoRI restrictions sites. Amino acid sequence of the human P2X₄ receptors fully corresponds to the isoform 3 described in gene database of the National Institute of Health.

Cell culture and establishment pmCherry-N1-hP2X₄ expressing HEK 293 cell clones

Human embryonic kidney (HEK) 293 cells were grown in plastic tissue culture flasks in DMEM/Ham's F-12 (1:1) medium supplemented with 5% fetal bovine serum, 100 U/ml penicillin and 100 µg/ml streptomycin at 37°C in a cell culture incubator supplied with 5% CO₂. Cells were subcultivated when confluency reached 90-95%. To establish pmCherry-N1-hP2X₄ expressing HEK 293 cell clones, cells plated the day before on poly-D-lysine coated 35 mm dish were transfected with 2 µg pmCherry-N1-hP2X₄ using 5 µl Lipofectamine 2000 per well as described in the manufacturer's protocol. Transfection medium was changed to antibiotic-free medium after 4 hours. On the following day the medium was then changed with selection antibiotic (G418) containing medium. From then on, the cells were kept in this selection medium. After a massive cell death of the non-transfected cells, surviving cells were trypsinized and replated in a 96-well plate at such a dilution that 1 cell/well density was obtained. After several days, colonies of cells displaying red fluorescence were selected as hP2X₄-expressing positive clones using fluorescence microscopy.

Transient transfection

Before the day of transfection, cells were plated on poly-D-lysine coated round glass coverslips (25 mm in diameter) at a density of 500,000 cells in 40 mm plastic Petri dishes. After 16-24 h, cells were transfected with 3 µg pmCherry-N1-hP2X₄ DNA and 5 µl of TurboFect™ transfection reagent in 200 µl of serum-free medium. Cells were subjected to experiments 16-48 h after transfection. The efficiency of transfection was 60-70%.

Cell surface biotinylation and western blotting

P2X₄ expressing HEK 293 cell clones were plated at 1.000.000 cell density into poly-D-lysine coated 60 mm dishes. 24 hours after plating, cells were rinsed with ice-cold PBS-Ca-Mg (PBS containing 0.1 mM CaCl₂ and 1 mM MgCl₂) followed by biotinylation of proteins at the plasma membrane with 1.5 mg/ml sulfo-NHS-LC-biotin in 10 mM triethanolamine (pH 7.4), 1 mM MgCl₂, 2 mM CaCl₂, and 150 mM NaCl for 90 minutes with horizontal shaking at 4°C. Next, excess biotin was quenched with PBS containing 1 mM MgCl₂, 0.1 mM CaCl₂, and 100 mM glycine for 20 minutes at 4°C, and then rinsed three times with PBS. Cells were finally lysed in lysis buffer for 30 minutes and lysates were cleared by centrifugation. Protein concentrations were determined by DC Protein Assay. Portion of cell lysates of equivalent amounts of protein (1.33 mg/ml) were equilibrated overnight with streptavidin agarose beads at 4°C. Beads were washed sequentially with solutions A [50 mM Tris-HCl (pH 7.4), 100 mM NaCl, and 5 mM EDTA] three times, B [50 mM Tris-HCl (pH 7.4) and 500 mM NaCl] twice, and C (50 mM Tris-HCl, pH 7.4) once. Biotinylated surface proteins were then released by heating to 95°C with 4x Laemmli buffer. Proteins from the intracellular fraction were also heated to 95°C for 5 minutes with 4x Laemmli buffer.

Samples were run on a 10% SDS gel with 40 µl protein loaded from the cytosolic protein (1 mg/ml) and the plasma membrane samples. Samples were transferred onto a PVDF membrane in Towbin's buffer using the semi-dry transfer method. Membranes were blocked with PBS containing 5% milk, 0.5% BSA and 0.02% NaN₃ at room temperature for 1 hour. Afterwards, samples were incubated in blocking solution containing the appropriate primary antibody (1:1000 for mouse anti-mCherry (Clontech, 632543)) at 4°C for overnight followed by three washes with PBST. HRP-conjugated goat anti-mouse antibody (1:4000, BioRad) was used as secondary antibody. After three consecutive washes with PBST and a final wash

with PBS, the enhanced chemiluminescence (ECL) method was used for detection. For loading control the membrane probed with anti-mCherry was stripped and blotted with avidin-HRP (1:1000, BioRad).

Histochemistry

After 24 hours of plating 400.000 P2X₄-expressing HEK 293 clonal cells into a 35 mm dish, cells were washed thoroughly with PBS. Next, cells were incubated with 0.1 mg/ml LC-sulfo-NHS(+)-biotin (Molbio) at room temperature for 1 hour followed by three washes with PBS. Thereafter, cells were fixed with 4% PFA at 37°C for 15 minutes. Cells were washed three times with PBS before staining with Streptavidin conjugated to Alexa 488 (1:4000 dilution, Invitrogen) at room temperature for one hour. After washing the cells four times with PBS, samples were mounted with CitiFluor AF2 (EMS). Images were captured with a Nikon C1 confocal laser scanning microscopy system equipped with Multiline Argon and HeNe lasers using 40x magnification.

Measurement of intracellular calcium levels

Transiently transfected HEK 293 cells were loaded with Fluo-3/AM (4μl) in standard extracellular solution for 45 min at room temperature. Fluorescence dye was dissolved in DMSO containing 20% Pluronic-F127. Additionally, the loading solution contained 1 mM probenecid to prevent dye leakage. After dye loading, cells were washed with standard extracellular solution. Standard extracellular solution contained (in mM): 145 NaCl, 5 KCl, 2 CaCl₂, 1 MgCl₂, 10 D-glucose and 10 HEPES, pH 7.4 (with NaOH). Nominally Ca²⁺-free solutions were prepared by simply omitting CaCl₂.

Measurements were performed with a Axiovert 200 M Zeiss LSM 510 Meta (Carl Zeiss, Jena, Germany) confocal laser scanning microscope equipped with a 20x Plan Aplanachromat (NA=0.80) DIC objective. For the excitation, 488-nm argon-ion laser was used. The emitted light was collected with BP 505-570 band pass filter. Data were obtained at a rate of 0.5 Hz. Changes in [Ca²⁺]_i are displayed as the percentage of fluorescence relative to the intensity at the beginning of each experiment. The baseline fluorescence (100 %) was calculated from the average fluorescence of ROIs while bathing the cells with standard extracellular solution. Background fluorescence was subtracted from fluorescence intensity by measuring a cell-free area on every coverslip. Agonists and antagonists were administered directly to the solution at the desired concentrations. All experiments were done at room temperature (22-24 °C).

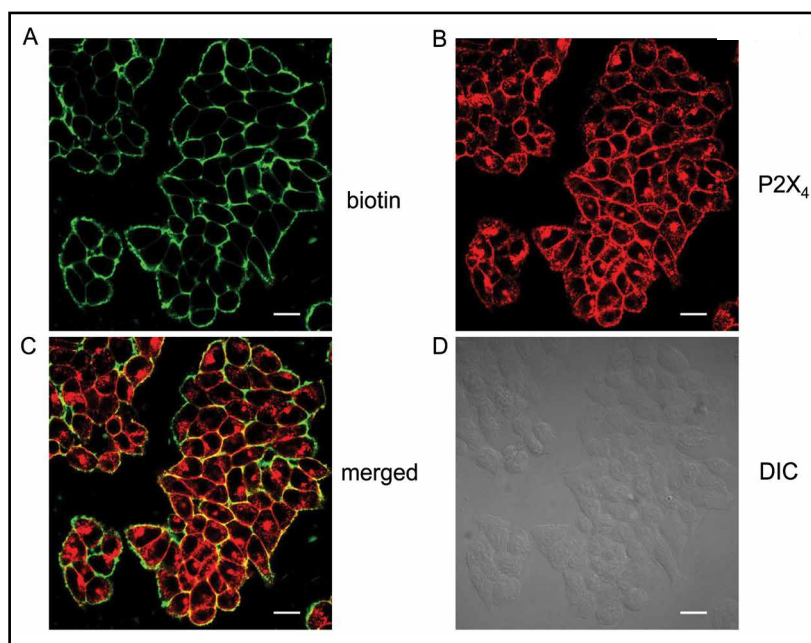
Fluorescence ion measurement experiments using FLIPRTetra

Cells were trypsinized and plated at 40,000 cells/well density in 100 μl volume onto 96-well black plates coated with 100μg/ml poly-D-lysine 36 hours before the experiments. HEK 293 cells were used for testing the effects of compounds on endogenous P2Y receptors; whereas P2X₄ activity was measured using P2X₄-expressing HEK 293 cell clones. 36 hours later the medium was replaced with 100 μl of loading buffer (modified Krebs buffer containing 117 mM NaCl, 4,8 mM KCl, 1 mM CaCl₂, 1 mM MgCl₂, 5 mM D-glucose, 10 mM HEPES, and Calcium-5 fluorescence dye). Cells were then incubated in the loading buffer at 37°C for one hour. Fluorescence calcium measurements were carried out using FLIPRTetra high-throughput, fluorescence microplate reader. Cells were excited using a 470-495 nm LED module, and the emitted fluorescence signal was filtered with a 515-575 nm emission filter. After establishment of a stable baseline, cells were incubated with the compounds for five minutes followed by the administration of ATP with or without the tested compounds.

Electrophysiology

Voltage-clamp recordings were carried out in the standard whole-cell configuration using an Axopatch 200B amplifier (Axon Instruments) [32]. Human P2X₄-expressing cells were selected using a Diaphot 300 inverted patch clamp microscope (Nikon) equipped with an epifluorescent attachment (Elektro-Optika, Érd, Hungary). Micropipettes were pulled by a P-97 Flaming-Brown type micropipette puller (Sutter Instrument) from borosilicate glass capillary tubes (Harvard Apparatus) and had a tip resistance of 3–6 MΩ when filled with pipette solution. Patch pipette filling solution contained (in mM): 135 KCl, 5 NaCl, 1 MgCl₂, 1 EGTA, 10 HEPES and an appropriate concentration of CaCl₂, to give free [Ca²⁺]_i = 0.1 μM. Free [Ca²⁺]_i was estimated using MaxChelator software (Stanford University, Palo Alto, USA). The pH was adjusted to 7.2 with KOH. Standard extracellular solution contained (in mM): 145 NaCl, 5 KCl, 2 CaCl₂, 1 MgCl₂, 10 D-glucose, 10 HEPES, pH 7.4 (with NaOH). Solutions were delivered by continuous perfusion with a gravity-fed delivery system. Antagonists were added to the bath solutions 3-5 min. prior to agonist application.

Fig. 1. Cellular localization of P2X₄Rs by immunohistochemistry. Panel A: Cell surface proteins stained with LC-sulfo-NHS(+)-biotin and streptavidin-Alexa488. Panel B: Fluorescence image of mCherry tagged P2X₄Rs in HEK 293 cells. Panel C: Merged image showing co-localization of P2X₄Rs and biotinylated cell surface proteins. Panel D: Differential interference contrast (DIC) image of the P2X₄Rs expressing cells. Scale bar represents 20 μ m.



Experiments were performed at a holding potential of -60 mV. Command protocols and data acquisition were controlled by pClamp 6.03 software (Axon Instruments). Capacitative currents were compensated with analog compensation. Series resistance was accepted if lower than five times the pipette tip resistance. Analog data were filtered at 1 kHz with a low-pass Bessel filter and digitized at 5 kHz using a Digidata 1200 interface board. Data were analyzed using Clampfit 6.03 and Microsoft Excel softwares. All experiments were performed at room temperature.

Data presentation

Areas under the curve (AUC) values were calculated using the trapezoidal rule, in the first 4 minutes following agonist application (SigmaPlot 12.0 software). To estimate P2X receptor function, non-expressing cell responses were subtracted from the AUC values obtained in P2X₄R expressing cells on the same coverslip.

Antagonist concentration-inhibition curves were obtained by using progressively increasing antagonist concentrations and a fixed agonist concentration close to the EC₅₀ unless otherwise stated. IC₅₀ values were calculated by least squares fitting to $I = I_0 / [1 + (IC_{50} / [Ant])^{-nH}]$, where I and I₀ represent peak responses in the presence and absence of antagonist at concentration [Ant].

Results were presented as means \pm SEM of n observations if not otherwise indicated. Statistical significance was determined using paired Student's t-test for parametric, whereas one-way ANOVA followed by Mann-Whitney U test for non-parametric variables. Differences were considered statistically significant when $p < 0.05$. Non-linear curve fitting was performed using the SigmaPlot 12.0 program.

Results

Localization and functional characterization of transfected hP2X₄ receptors in HEK 293 cells

In order to study the localization of transfected hP2X₄ receptors in HEK 293 cells we used immunohistochemical techniques. Co-localization of biotinylated cell surface proteins and mCherry fluorescent protein suggested the expression of P2X₄Rs in the plasma membrane (Fig. 1). Furthermore, cell surface biotinylation and western blotting were used to separate the cytosolic and membrane fractions of proteins in HEK 293 cells. The P2X₄-bound mCherry protein was detected at the plasma membrane and its expression was not altered by the presence of ivermectin (Fig. 2A). In control experiment we used avidin-HRP-conjugated antibody to confirm the localization of proteins in the membrane fraction (Fig. 2B).

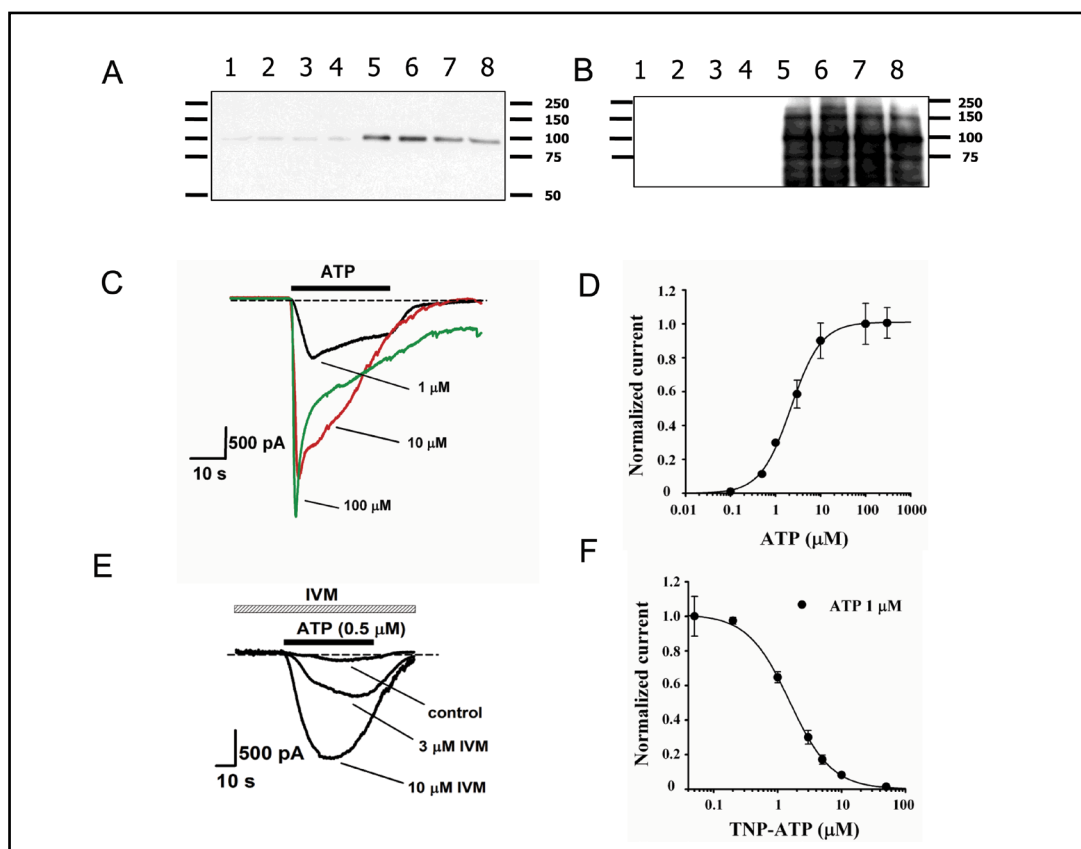


Fig. 2. Localization and functional characterization of transfected hP2X₄ receptors in HEK 293 cells. Panel A: Cytosolic and cell surface proteins were separated. Human P2X₄Rs are expressed both in cytosolic (lanes 1-4) and plasma membrane (lanes 5-8) fractions of proteins. Lane 1 and 5 indicate unstimulated cells, lanes 2 and 6 DMSO-pretreated (1:1000) cells, lanes 3 and 7 IVM-pretreated (10 μM) cells and lanes 4 and 8 IVM-pretreated (20 μM) cells. Panel B: In control experiments we obtained protein expression only in cell surface fraction (lanes 5-8) using avidin-HRP. Panel C: Representative traces showing ATP-induced inward currents in the absence; and panel E: presence of ivermectin (IVM). Panel D: Concentration-responses to ATP (0.1-300 μM) are shown. Panel F: Concentration-inhibitions to TNP-ATP (0.05-50 μM) in ATP-stimulated (1 μM) cells are shown. Values are means ± SEM. The error bars are not always visible due to the small SEM values. Experiments at each concentration were performed at least 3 times.

To functionally characterize the plasma membrane localized hP2X₄ receptors we measured whole cell currents in transfected HEK 293 cells. ATP (0.1-300 μM) elicited increasing maximal current amplitudes in cells expressing P2X₄Rs (Fig. 2C and D). The agonist concentration-response curve for ATP were fit with the Hill-equation; $E = E_{\max} [1 + (EC_{50}/[A])^{nH}]^{-1}$ where E stands for the peak current evoked by agonist concentration $[A]$, E_{\max} is the peak current evoked by a maximal agonist concentration, EC_{50} is the concentration giving half the maximal current, and nH represents the Hill coefficient. Our results showed that the EC_{50} value of ATP was 2.1 μM (Fig. 2D). Cells lacking P2X₄R expression failed to respond to ATP (100 μM) (data not shown). To confirm the role of P2X₄Rs in ATP-induced inward currents we pretreated the cells with ivermectin (IVM) (3 and 10 μM). As expected, IVM potentiated currents induced by ATP (0.5 μM) in a concentration-dependent manner (Fig. 2E). In addition, we tested the effects of TNP-ATP on ATP-induced (1 μM) currents. Under these conditions, we found that the half-maximal inhibitory concentration (IC_{50}) of TNP-ATP was 1.5 μM (Fig. 2F). These data show the plasma membrane localized hP2X₄ receptors are fully functional in transfected HEK 293 cells.

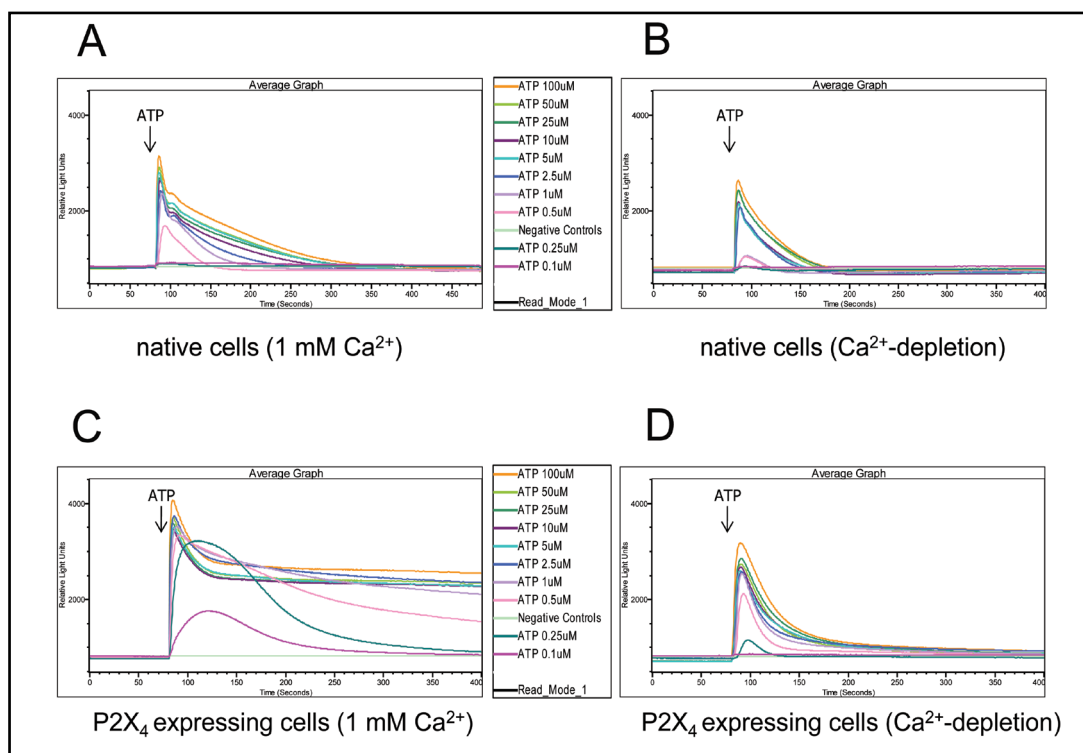


Fig. 3. ATP-induced changes of cytosolic calcium concentration measured using FLIPRTetra. Panels A and B: Administration of extracellular ATP induced dose-dependent, similar transient changes of cytosolic calcium in HEK 293 cells in the presence or absence of extracellular calcium. Panel C: In contrast, in HEK 293 cells stably expressing hP2X₄ ATP-induced sustained calcium response in the presence of extracellular calcium. Panel D: whereas in calcium-free buffer the responses were similar to the ones obtained in non-transfected cells. Average tracings of 6 individual experiments are shown.

ATP-induced Ca²⁺ influx is inhibited by 5-BDBD in cells stably expressing P2X₄Rs

In native HEK 293 cells ATP (0.5–100 μM) caused transient increases in cytosolic calcium concentrations whereas lower doses of the agonist (0.1–0.25 μM) elicited no change in calcium levels (Fig. 3A). In nominally calcium-free buffer ATP (0.1–100 μM) caused similar effects suggesting that the calcium signal was due to P2Y receptor-dependent Ca²⁺ release from the intracellular stores (Fig. 3B). Although the presence of external Ca²⁺ prolonged ATP-induced calcium signals, sustained responses could not be observed (Fig. 3A). Next, we studied ATP-induced Ca²⁺ signals in HEK 293 cell clones stably expressing P2X₄Rs (see methods). In these cells ATP (0.1–0.25 μM) elicited changes in Ca²⁺ concentrations that were abolished in Ca²⁺-depleted medium indicating that Ca²⁺ entered the cells from the extracellular space (Fig. 3C and D). In addition, higher concentrations of ATP (≥ 1 μM) caused sustained Ca²⁺ signals (Fig. 3C). Importantly, the P2X₄ receptor-specific positive allosteric modulator IVM (20 μM) potentiated the ATP-induced (0.25 μM) Ca²⁺ entry ($AUC_{ATP} = 852 \pm 47$; $n=5$ vs. $AUC_{ATP+IVM} = 1026 \pm 46$; $n=5$; $p<0.05$). These data indicate that using low concentrations of ATP (≤ 0.25 μM) allows assessment of P2X₄R-mediated Ca²⁺ signals independent of P2Y receptor activation. Thus, we next studied the effects of the benzodiazepine derivative 5-BDBD in the presence of 0.25 μM ATP. Under these conditions 5-BDBD (2–20 μM) significantly inhibited P2X₄R-mediated Ca²⁺ entry (Fig. 4A). We obtained similar inhibitory effects of 5-BDBD when cells were stimulated by 0.5 μM ATP (Fig. 4B). Regardless of ATP concentrations used, 5-BDBD (1–20 μM) had no effects in native HEK 293 cells suggesting that endogenously expressed P2Y receptors were not inhibited (data not shown).

Fig. 4. 5-BDBD inhibited the ATP-induced Ca²⁺ signals in HEK 293 cells stably expressing hP2X₄ receptors. Panels A and B: Concentration-dependent inhibition of Ca²⁺ signals by 5-BDBD when cells were stimulated with 0.25 μM and 0.5 μM ATP. Values are means ± SD. Each experiment was performed at least 4 times. A.U. means arbitrary units. *p<0.05 and **p<0.005 vs. ATP positive controls (ANOVA).

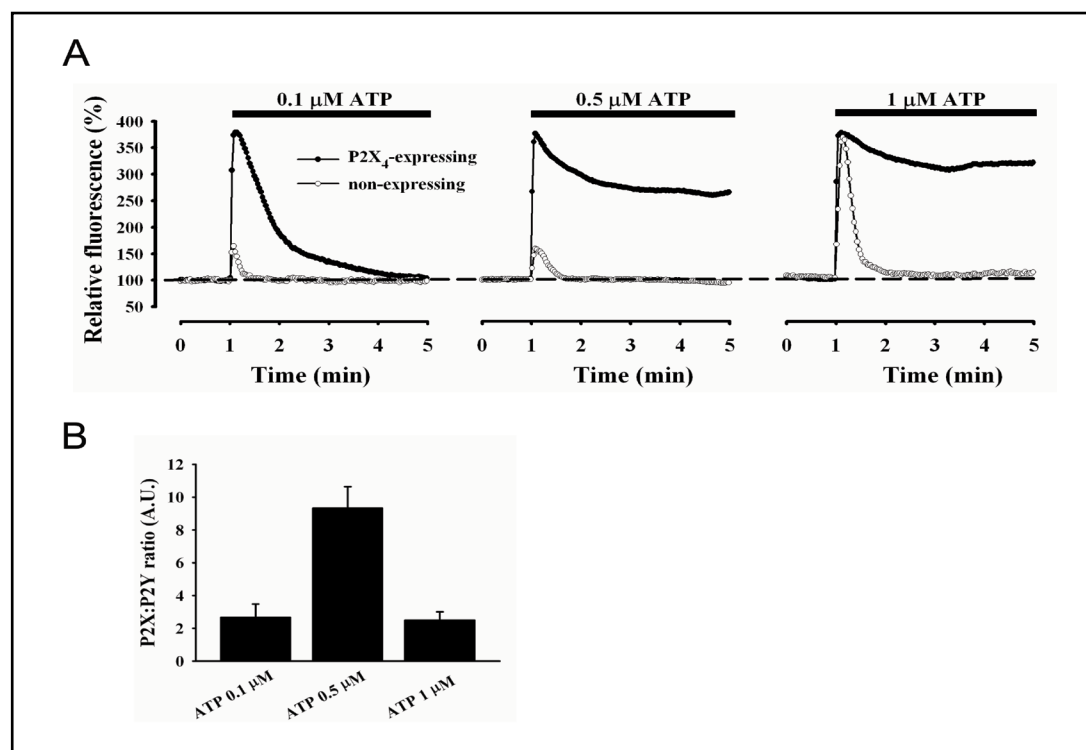
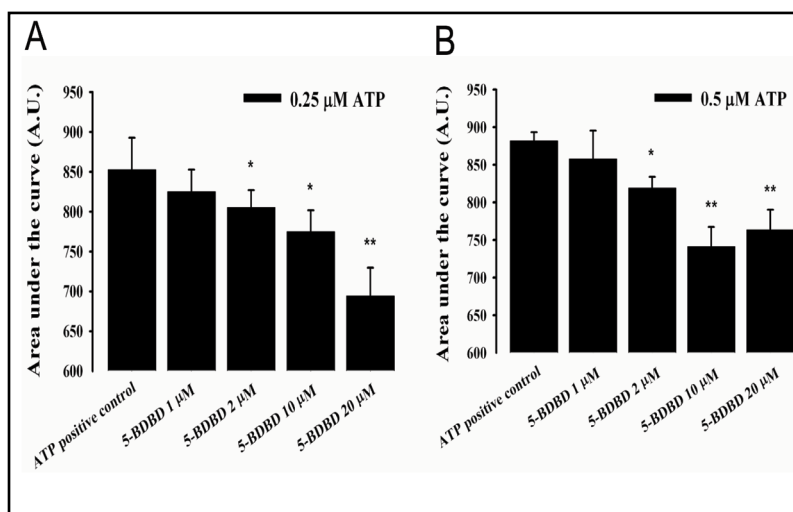
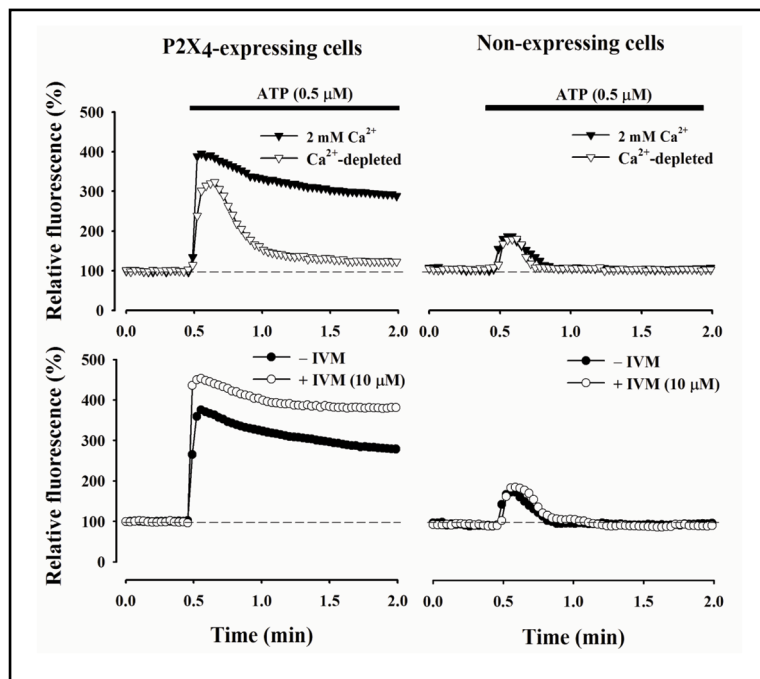


Fig. 5. ATP induced concentration-dependent changes in [Ca²⁺]_i in hP2X₄-expressing and non-expressing HEK 293 cells. Panel A: Representative traces showing the effects of different ATP concentrations (0.1–1 μM) on [Ca²⁺]_i. Each experiment was performed at least 5 times; Panel B: P2XR:P2Y-mediated Ca²⁺ response ratios are shown at different ATP concentrations. P2YR-mediated responses were estimated by the amplitude of cytosolic Ca²⁺ peaks while P2XR-mediated responses were assessed by “area under the curve” (AUC) values referring to the sustained nature of the Ca²⁺ signal. S.E.M. values are not shown for the representative traces because they were within 10% of the mean. A.U. means arbitrary units.

Single cell calcium imaging in cells transiently expressing P2X₄Rs

Single cell calcium imaging has been shown to provide an alternative method for the assessment of P2X receptor channel activity [33]. Therefore, we also studied the ATP-induced intracellular Ca²⁺ signals at the single cell level. In order to conduct simultaneous measurements of cytosolic Ca²⁺ levels in P2X₄R-expressing and non-expressing cells, we used

Fig. 6. Top panels: ATP induced changes in $[Ca^{2+}]_i$ in Ca^{2+} -containing or Ca^{2+} -depleted medium. Bottom panels: Ivermectin (IVM) potentiated the ATP-induced Ca^{2+} signal only in hP2X₄-expressing cells.



the transient transfection method. First, we identified the extracellular ATP concentration at which P2XR:P2YR-mediated Ca^{2+} response ratio was the highest. The P2YR-mediated responses were estimated by the amplitude of cytosolic Ca^{2+} peaks while P2XR-mediated responses were assessed by “area under the curve” (AUC) values referring to the sustained nature of the Ca^{2+} signal. In cells lacking P2X₄R expression, administration of 0.1 μM and 0.5 μM ATP evoked small peak increases without sustained Ca^{2+} signals (Fig. 5A). In cells expressing P2X₄Rs, the magnitude of Ca^{2+} peaks induced by 0.1 μM and 0.5 μM ATP were significantly higher than in non-expressing cells. However, robust Ca^{2+} plateau was induced only by 0.5 μM ATP (Fig. 5A). Further increasing ATP concentrations (1 μM), a considerable rise in cytosolic Ca^{2+} peak was observed in cells lacking P2X₄R expression. In contrast, the sustained component of the Ca^{2+} signal induced by 1 μM ATP did not significantly differ from that elicited by 0.5 μM ATP in P2X₄R expressing cells (Fig. 5A). Consequently, as P2XR:P2YR-mediated Ca^{2+} response ratio was the highest at 0.5 μM ATP (Fig. 5B), in subsequent experiments this concentration was chosen to investigate single cell Ca^{2+} signals. To demonstrate that extracellular Ca^{2+} was necessary for ATP-induced sustained Ca^{2+} signal in cells expressing P2X₄Rs, we repeated the experiments in Ca^{2+} -depleted medium. Under these circumstances, the Ca^{2+} signal was only transient suggesting that Ca^{2+} entry was due to functional expression of P2X₄Rs (Fig. 6). In cells lacking P2X₄R expression, external Ca^{2+} did not influence the ATP-induced transient nature of cytosolic Ca^{2+} signal (Fig. 6). These data excluded the possibility that store-operated calcium channels played significant role in Ca^{2+} entry when cells were stimulated with 0.5 μM ATP. To further characterize the sustained Ca^{2+} signal, we pretreated the cells with IVM (10 μM) 5 min prior the application of ATP. Our results showed that ATP-induced Ca^{2+} plateau was significantly elevated in P2X₄R expressing but not in non-expressing cells (Fig. 6).

Next, we tested the effects of 5-BDBD on ATP-induced (0.5 μM), P2X₄R-mediated Ca^{2+} entry. Sustained Ca^{2+} signals were diminished in cells pretreated with different concentrations of 5-BDBD (0.5–20 μM). We observed 50% reduction of the AUC values in the presence of approx. 2 μM 5-BDBD (Fig. 7A). We also studied inhibitory effects of TNP-ATP which was reported as a putative antagonist of P2X₄Rs [25]. As shown in Figure 7B, TNP-ATP (0.5–50 μM) reduced ATP-induced (0.5 μM) sustained Ca^{2+} signal in a concentration-dependent manner. Taken together, these data indicate that ATP-induced sustained Ca^{2+} signals were inhibited by both 5-BDBD and TNP-ATP in HEK 293 cells transfected with P2X₄Rs.

Fig. 7. Both 5-BDBD and TNP-ATP inhibited the ATP-induced Ca²⁺ signals in HEK 293 cells transiently transfected with hP2X₄ receptors. Panels A and B: Concentration-dependent inhibition of the ATP-induced Ca²⁺ response by 5-BDBD (0.5–20 μM); and TNP-ATP (0.5–50 μM). The number of independent experiments is indicated in parenthesis beneath the columns.

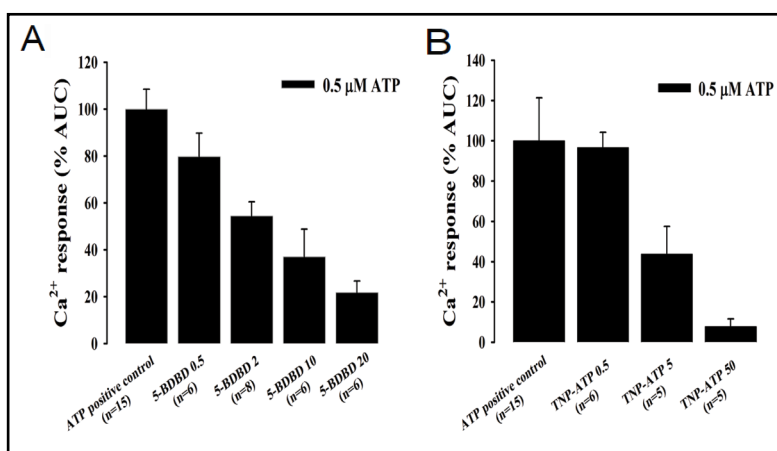
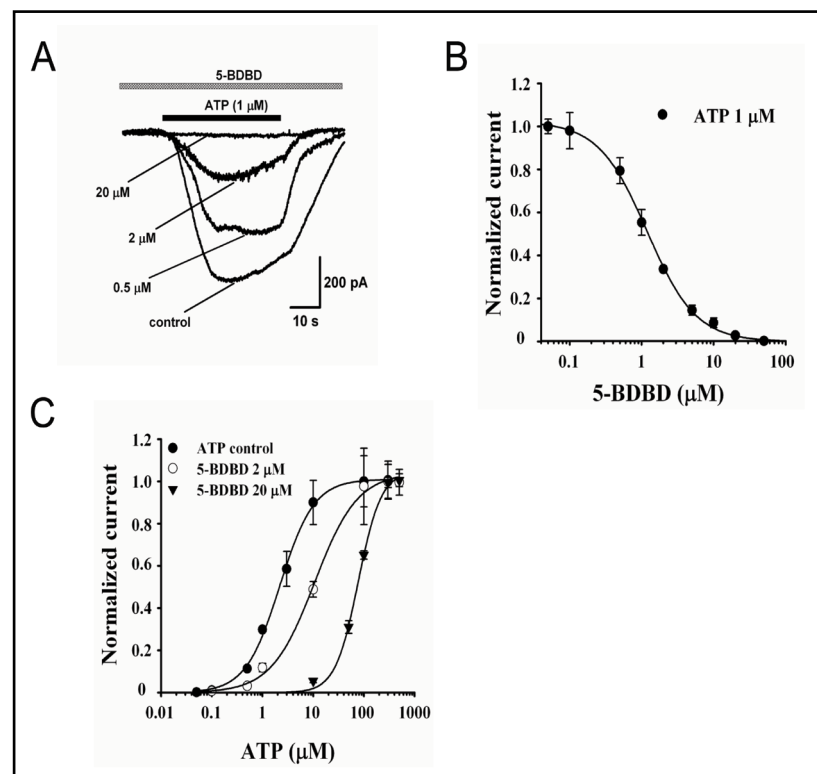


Fig. 8. 5-BDBD competitively inhibited the ATP-induced whole cell inward ion currents in HEK 293 cells transiently expressing hP2X₄ receptors. Panel A: Representative original traces showing the inhibitory effects of 5-BDBD at various concentrations. Panel B: Concentration-dependent inhibition of 5-BDBD (0.1–50 μM) in ATP-stimulated (1 μM) cells are shown. Panel C: Concentration-dependent responses to ATP (0.1–300 μM) in cells that were pretreated with 2 or 20 μM 5-BDBD. The rightward shift of the ATP control curve and the unchanged maximal stimulation suggest that 5-BDBD competitively inhibited the P2X₄ receptor channels. In the absence of 5-BDBD the Hill coefficient was 1.26. In the presence of 2 μM and 20 μM 5-BDBD nH values were 1.11 and 2.17, respectively. Values are means ± SEM. The error bars are not always visible due to the small SEM values. Experiments at each concentration were performed at least 3 times.



stimulation suggest that 5-BDBD competitively inhibited the P2X₄ receptor channels. In the absence of 5-BDBD the Hill coefficient was 1.26. In the presence of 2 μM and 20 μM 5-BDBD nH values were 1.11 and 2.17, respectively. Values are means ± SEM. The error bars are not always visible due to the small SEM values. Experiments at each concentration were performed at least 3 times.

P2X₄ receptor channels are competitively inhibited by 5-BDBD

Data presented in this paper show that 5-BDBD inhibited the P2X₄R-mediated Ca²⁺ entry in both stably and transiently transfected HEK 293 cells (see above). Nonetheless, during measurements of intracellular Ca²⁺ concentrations activation of endogenous P2YRs and/or ion transporters that eliminate Ca²⁺ from the cytosol (i.e. plasma membrane Ca²⁺-ATPase, sarcoplasmic reticulum Ca²⁺-ATPase) might possibly interfere with the effectiveness of 5-BDBD. Therefore, we also tested the inhibitory effects of 5-BDBD in HEK 293 cells using the whole cell configuration of the patch clamp technique. We stimulated the cells with 1 μM

ATP (close to EC₃₀ of ATP) because higher concentrations of the agonist induced premature cell damage in a number of experiments. Under these circumstances, 5-BDBD (0.1-50 μM) dose-dependently inhibited P2X₄R-mediated inward currents (I_{control} : 1239 ± 105 pA, n=8 vs. $I_{0.5\mu\text{M}}$: 983 ± 148 pA, n=4 vs. $I_{2\mu\text{M}}$: 417 ± 33, n=4 vs. $I_{20\mu\text{M}}$: 13 ± 1 pA, n=4) with an IC₅₀ of 1.2 μM (Fig. 8A and B). To investigate whether the inhibitory effect of 5-BDBD was due to competitive or allosteric interaction with P2X₄Rs, we performed additional electrophysiological experiments. Application of two different concentrations of 5-BDBD (2 μM and 20 μM) caused a rightward shift in ATP dose-response curve (from EC₅₀ = 2.1 μM to 11.2 μM and 79.2 μM, respectively, using non-linear regression analysis). Since the magnitude of maximal stimulation did not change, these data suggest that 5-BDBD competitively inhibited the P2X₄Rs (Fig. 8C).

Discussion

P2X₄ receptors are involved in important physiological and pathophysiological functions such as afferent signalling, chronic pain and autocrine/paracrine communications of endothelial and epithelial cells. In these processes, investigations on the role of P2X₄Rs are often hindered by lack of selective inhibitors. In recent years, considerable efforts have been made to discover novel effective antagonists of P2X₄Rs. Although the benzodiazepine derivative 5-BDBD has been recently proposed to selectively block P2X₄Rs [27], only limited experiences have been available concerning its inhibitory properties [28-31]. Moreover, to the best of our knowledge, there are no previous studies attempting to compare the inhibitory effects of 5-BDBD using both electrophysiological and intracellular calcium measurements. Therefore, we aimed to investigate the inhibitory potency of 5-BDBD on P2X₄R-dependent Ca²⁺ entry. Our data provide evidence for competitive though moderate inhibitory effects of 5-BDBD. Depending on experimental conditions the degree of inhibition varied significantly. In patch clamp experiments, assessing the effects of 5-BDBD directly on its target protein, we obtained the strongest inhibition. In intracellular calcium measurements, 5-BDBD exhibited more robust effects in transiently transfected cells. This was probably due to both the higher level of P2X₄R expression and the single cell calcium measurements. However, it is important to emphasize that AUC values are not in a linear fashion with [Ca²⁺]_i and quantitative analyses of fluorometric Ca²⁺ assay may provide only a rough orientation.

Despite the endogenous expression of at least three different P2Y receptor subtypes [34, 35] HEK 293 cells are frequently used to study properties of P2X receptors [34, 36]. To assess the role of P2XRs in inducing changes of intracellular Ca²⁺ concentrations, some investigators often choose cell lines (i.e. excitable mouse immortalized gonadotropin-releasing hormone-secreting cells (GT1) and human astrocytoma cells (1321N1)) that are lacking P2Y receptors [33, 37]. Stojilkovic and his colleagues transfected both GT1 and HEK 293 cells with different P2X subtypes and compared ATP-induced Ca²⁺ signals. They concluded that intracellular Ca²⁺ measurements could be used for the characterization of P2X receptors only in GT1 but not in HEK 293 cells because activation of endogenously expressed P2Y receptors interferes with P2X receptor-mediated Ca²⁺ signals [33]. This is indeed the case when HEK 293 cells are stimulated with high concentrations of ATP (>10 μM). Nonetheless, here we propose an alternative approach to investigate P2XR functions in HEK 293 cells applying low doses of agonist. In the present study, we show that submicromolar concentrations of ATP (≤ 0.25 μM) cause changes in intracellular Ca²⁺ concentrations solely in P2X₄R expressing cells. The ATP-induced increase in Ca²⁺ concentrations was further enhanced by pretreatment of ivermectin and was completely abolished in Ca²⁺-depleted medium suggesting that P2X₄Rs were involved in Ca²⁺ influx. Furthermore, we found that higher doses of ATP (≥1 μM) prolonged the duration of Ca²⁺ signals in native HEK 293 cells. These effects were abolished in Ca²⁺-depleted medium suggesting the activation of P2X₄R-independent Ca²⁺ influx mechanisms. The significantly higher initial phase of Ca²⁺ response in P2X₄R expressing cells compared to native cells was probably due to the fact that we used

nominally Ca²⁺ free solutions. Nonetheless, according to our previous experience, we could not add calcium chelators because HEK 293 cells require extracellular Ca²⁺ to remain attached to the coverslip. We assume that, as a result of P2Y receptor-dependent Ca²⁺ release, store-operated Ca²⁺ entry could contribute to the overall Ca²⁺ signal when cells are stimulated with higher concentrations of ATP (>1 μM). Therefore, our results suggest that when sufficiently low ATP concentrations are applied, measurement of intracellular Ca²⁺ concentrations is a useful approach to assess properties of P2XR in HEK 293 cells.

Considering the fact that Ca²⁺ measurement in stably transfected cells did not allow concurrent investigations of the P2X₄R-expressing and non-expressing cells, we also performed single cell calcium measurements in transiently transfected HEK 293 cells. Thus, we could simultaneously measure ATP-induced Ca²⁺ signals in P2X₄R-expressing and non-expressing cells on the same coverslip. Our data suggest that up to the concentration of 0.5 μM, ATP causes only small transient changes in Ca²⁺ concentration whereas 1 μM ATP significantly enhances the signal amplitude in non-expressing cells. This phenomenon was probably due to the gradual activation of different endogenous P2Y receptor subtypes [35].

To our surprise, we found that amplitudes of ATP-induced Ca²⁺ signals were significantly higher in P2X₄R-expressing than in non-expressing cells when experiments were performed in Ca²⁺-depleted medium (Fig. 6). Since we obtained similar results in stably transfected cells as well, we speculate that the difference was due to P2X₄R-mediated Ca²⁺ entry rather than additional release of Ca²⁺ from the internal stores. High levels of P2X₄R-expression and lack of Ca²⁺-chelation could both contribute to the Ca²⁺ entry. Furthermore, our data show that IVM enhances the ATP-induced Ca²⁺ entry only in P2X₄R-expressing cells. In accordance with previous observations, IVM potentiated ATP-induced Ca²⁺ entry but did not increase surface expression of P2X₄Rs [38, 39].

Our electrophysiological data confirmed the presence of functional P2X₄Rs in transiently transfected HEK 293 cells. ATP caused IVM-sensitive activation of inward currents in P2X₄R-expressing but not in non-expressing cells. We found EC₅₀ value of ATP close to what was previously reported [26]. However, it is noteworthy that, in some experiments ATP-stimulated currents exhibited incomplete recovery following withdrawal of the agonist when its concentration was higher than 1 μM. This was probably due to the high level of P2X₄R expression and massive Ca²⁺ influx which could consequently cause cellular damage. Therefore, inhibitory properties of both TNP-ATP and 5-BDBD were tested at 1 μM ATP stimulation.

Activation of P2X₄Rs plays a key role in the pathogenesis of neuropathic pain [15]. In an attempt to mitigate the neuropathic pain Inoue and his colleagues investigated the possible role of antidepressants as inhibitors of P2X₄Rs [37]. They found that paroxetine inhibited P2X₄Rs dose-dependently. Paroxetine behaved as a noncompetitive antagonist with IC₅₀ values of 2.5 μM and 1.9 μM for rat and human P2X₄Rs, respectively. Interestingly, inhibitory effects of paroxetine were significantly stronger on rat P2X₄Rs than that of TNP-ATP [37]. It is known that TNP-ATP is more than 1,000-fold more potent in blocking P2X₁ and P2X₃ than P2X₄ receptors [24]. Nonetheless, TNP-ATP has been used as P2X₄ antagonist in a number of studies [40, 41]. Our data also demonstrate that TNP-ATP inhibits both intracellular Ca²⁺ signals and inward ion currents induced by ATP. We found that TNP-ATP had an IC₅₀ value of 1.5 μM for 1 μM ATP stimulation which was comparable with previous observations [25]. Noncompetitive antagonism of TNP-ATP at the P2X₃Rs suggests similar mechanisms of action at P2X₄Rs as well [25].

Recently, 5-BDBD has been proposed to selectively inhibit P2X₄Rs [27]. Since then 5-BDBD has been used in a number of studies with contradictory results [28-31]. It has weak potency to inhibit recombinant human P2X₄Rs [28] or native P2X₄Rs in vascular endothelial cells (IC₅₀ ~ 30 μM) [30]. In contrast, P2X₄Rs were potently blocked by 10 μM 5-BDBD in prechondrogenic cell line [29]. Here we report that 5-BDBD and TNP-ATP have similar inhibitory potencies at recombinant human P2X₄Rs expressed in HEK 293 cells. Our data suggest that 5-BDBD may competitively inhibit the P2X₄Rs. However, we cannot exclude the possibility that 5-BDBD decreases the ligand-binding affinity of the channels. Such allosteric

alterations of ATP-binding affinity have been previously reported for P2X receptors [42, 43].

In conclusion, the present study demonstrates that intracellular measurement of Ca²⁺ concentration in HEK 293 cells could be a useful method to investigate pharmacological properties of P2X receptor antagonists provided that submicromolar concentrations of ATP are used. 5-BDBD and TNP-ATP have similar inhibitory potencies at human recombinant P2X₄Rs. Our data show that 5-BDBD shifts the ATP concentration-response curve to the right. This feature differs from the previously described noncompetitive behavior of other P2X₄R antagonists such as TNP-ATP and paroxetine.

Acknowledgements

This work was supported by the OTKA K79189 grant and Swiss National Science Foundation (SNSF) through the National Centre of Competence in Research (NCCR) TransCure (website: <http://www.transcure.org>). The authors thank Péter Várnai and Dániel Tóth for their help to create the pmCherry-N1-hP2X₄ construct.

References

- 1 Schwiebert EM, Zsembery A: Extracellular ATP as a signaling molecule for epithelial cells, *Biochim Biophys Acta* 2003;1615:7-32.
- 2 Burnstock G, Fredholm BB, North RA, Verkhratsky A: The birth and postnatal development of purinergic signalling. *Acta Physiol* 2010;199:93-147.
- 3 Jo YH, Role LW: Coordinate release of ATP and GABA at in vitro synapses of lateral hypothalamic neurons. *J Neurosci* 2002;22:4794-4804.
- 4 Sim JA, Chaumont S, Jo J, Ulmann L, Young MT, Cho K, Buell G, North RA, Rassendren F: Altered hippocampal synaptic potentiation in P2X₄ knock-out mice. *J Neurosci* 2006;26:9006-9009.
- 5 Khakh BS, Kennedy C: Adenosine and ATP: Progress in their receptors' structures and functions. *Trends Pharmacol Sci* 1998;19:39-41.
- 6 Roper SD: Signal transduction and information processing in mammalian taste buds. *Pflugers Arch* 2007;454:759-776.
- 7 Housley GD, Marcotti W, Navaratnam D, Yamoah EN: Hair cells--beyond the transducer. *J Membr Biol* 2006;209:89-118.
- 8 Rong W, Gourine AV, Cockayne DA, Xiang Z, Ford AP, Spyer KM, Burnstock G: Pivotal role of nucleotide P2X₂ receptor subunit of the ATP-gated ion channel mediating ventilatory responses to hypoxia. *J Neurosci* 2003;23:11315-11321.
- 9 Di Virgilio F: Purinergic signalling in the immune system. A brief update. *Purinergic Signal* 2007;3:1-3.
- 10 Surprenant A, North RA: Signaling at purinergic P2X receptors. *Annu Rev Physiol* 2009;71:333-359.
- 11 Barclay J, Patel S, Dorn G, Wotherspoon G, Moffatt S, Eunson L, Abdel'al S, Natt F, Hall J, Winter J, Bevan S, Wishart W, Fox A, Ganju P: Functional downregulation of P2X₃ receptor subunit in rat sensory neurons reveals a significant role in chronic neuropathic and inflammatory pain. *J Neurosci* 2002;22:8139-8147.
- 12 Cockayne DA, Dunn PM, Zhong Y, Rong W, Hamilton SG, Knight GE, Ruan HZ, Ma B, Yip P, Nunn P, McMahon SB, Burnstock G, Ford AP: P2X₂ knockout mice and P2X₂/P2X₃ double knockout mice reveal a role for the P2X₂ receptor subunit in mediating multiple sensory effects of ATP. *J Physiol* 2005;567:621-639.
- 13 Coull JA, Beggs S, Boudreau D, Boivin D, Tsuda M, Inoue K, Gravel C, Salter MW, De Koninck Y: BDNF from microglia causes the shift in neuronal anion gradient underlying neuropathic pain. *Nature* 2005;438:1017-1021.
- 14 Chizh BA, Illes P: P2X receptors and nociception. *Pharmacol Rev* 2001;53:553-568.
- 15 Tsuda M, Shigemoto-Mogami Y, Koizumi S, Mizokoshi A, Kohsaka S, Salter MW, Inoue K: P2X₄ receptors induced in spinal microglia gate tactile allodynia after nerve injury. *Nature* 2003;424:778-783.
- 16 Labasi JM, Petrushova N, Donovan C, McCurdy S, Lira P, Payette MM, Brissette W, Wicks JR, Audoly L, Gabel CA: Absence of the P2X₇ receptor alters leukocyte function and attenuates an inflammatory response. *J Immunol* 2002;168:6436-6445.
- 17 Mulryan K, Gitterman DP, Lewis CJ, Vial C, Leckie BJ, Cobb AL, Brown JE, Conley EC, Buell G, Pritchard CA, Evans RJ: Reduced vas deferens contraction and male infertility in mice lacking P2X₁ receptors. *Nature* 2000;403:86-89.

- 18 Yamamoto K, Korenaga R, Kamiya A, Qi Z, Sokabe M, Ando J: P2X₄ receptors mediate ATP-induced calcium influx in human vascular endothelial cells. *Am J Physiol Heart Circ Physiol* 2000;279:H285-292.
- 19 Yamamoto M, Jin JJ, Wu Z, Abe M, Tabara Y, Nagai T, Yamasaki E, Igase M, Kohara K, Miki T, Nakura J: Interaction between serotonin 2A receptor and endothelin-1 variants in association with hypertension in Japanese. *Hypertens Res* 2006;29:227-232.
- 20 Ma W, Korngreen A, Weil S, Cohen EB, Priel A, Kuzin L, Silberberg SD: Pore properties and pharmacological features of the P2X receptor channel in airway ciliated cells. *J Physiol* 2006;571:503-517.
- 21 Zsembery A, Fortenberry JA, Liang L, Bebok Z, Tucker TA, Boyce AT, Braunstein GM, Welty E, Bell PD, Sorscher EJ, Clancy JP, Schwiebert EM: Extracellular zinc and ATP restore chloride secretion across cystic fibrosis airway epithelia by triggering calcium entry. *J Biol Chem* 2004;279:10720-10729.
- 22 Liang L, Zsembery A, Schwiebert EM: RNA interference targeted to multiple P2X receptor subtypes attenuates zinc-induced calcium entry. *Am J Physiol Cell Physiol* 2005;289:C388-396.
- 23 Doctor RB, Matzakos T, McWilliams R, Johnson S, Feranchak AP, Fitz JG: Purinergic regulation of cholangiocyte secretion: Identification of a novel role for P2X receptors. *Am J Physiol Gastrointest Liver Physiol* 2005;288:G779-786.
- 24 Gum RJ, Wakefield B, Jarvis MF: P2X receptor antagonists for pain management: Examination of binding and physicochemical properties. *Purinergic Signal* 2012;8:41-56.
- 25 Virginio C, Robertson G, Surprenant A, North RA: Trinitrophenyl-substituted nucleotides are potent antagonists selective for P2X₁, P2X₃, and heteromeric P2X_{2/3} receptors. *Mol Pharmacol* 1998;53:969-973.
- 26 Jarvis MF, Khakh BS: ATP-gated P2X cation-channels. *Neuropharmacology* 2009;56:208-215.
- 27 Fisher R, Grützmann R, Blasco HPJ, Kalthof B, Gadea PC, Stelte-Ludwig B, Woltering E, Wutke M: Benzofuro-1,4-diazepin-2-one derivatives. 2005; Patent Number: EP1608659A1
- 28 Norenberg W, Sobottka H, Hempel C, Plotz T, Fischer W, Schmalzing G, Schaefer M: Positive allosteric modulation by ivermectin of human but not murine P2X₇ receptors. *Br J Pharmacol* 2012;167:48-66.
- 29 Kwon HJ: Extracellular ATP signaling via P2X₄ receptor and cAMP/PKA signaling mediate ATP oscillations essential for prechondrogenic condensation. *J Endocrinol* 2012;214:337-348.
- 30 Wu T, Dai M, Shi XR, Jiang ZG, Nuttall AL: Functional expression of P2X₄ receptor in capillary endothelial cells of the cochlear spiral ligament and its role in regulating the capillary diameter. *Am J Physiol Heart Circ Physiol* 2011;301:H69-78.
- 31 Casati A, Frascoli M, Traggiai E, Proietti M, Schenk U, Grassi F: Cell-autonomous regulation of hematopoietic stem cell cycling activity by ATP. *Cell Death Differ* 2011;18:396-404.
- 32 Hamill OP, Marty A, Neher E, Sakmann B, Sigworth FJ: Improved patch-clamp techniques for high-resolution current recording from cells and cell-free membrane patches. *Pflugers Arch* 1981;391:85-100.
- 33 He ML, Zemkova H, Koshimizu TA, Tomic M, Stojilkovic SS: Intracellular calcium measurements as a method in studies on activity of purinergic P2X receptor channels. *Am J Physiol Cell Physiol* 2003;285:C467-479.
- 34 Fischer W, Wirkner K, Weber M, Eberts C, Koles L, Reinhardt R, Franke H, Allgaier C, Gillen C, Illes P: Characterization of P2X₃, P2Y₁ and P2Y₄ receptors in cultured HEK293-hP2X₃ cells and their inhibition by ethanol and trichloroethanol. *J Neurochem* 2003;85:779-790.
- 35 Fischer W, Franke H, Groger-Arndt H, Illes P: Evidence for the existence of P2Y_{1,2,4} receptor subtypes in HEK-293 cells: Reactivation of P2Y₁ receptors after repetitive agonist application. *Naunyn Schmiedeberg Arch Pharmacol* 2005;371:466-472.
- 36 Serrano A, Mo G, Grant R, Pare M, O'Donnell D, Yu XH, Tomaszewski MJ, Perkins MN, Seguela P, Cao CQ: Differential expression and pharmacology of native P2X receptors in rat and primate sensory neurons. *J Neurosci* 2012;32:11890-11896.
- 37 Nagata K, Imai T, Yamashita T, Tsuda M, Tozaki-Saitoh H, Inoue K: Antidepressants inhibit P2X₄ receptor function: A possible involvement in neuropathic pain relief. *Mol Pain* 2009;5:20.
- 38 Khakh BS, Proctor WR, Dunwiddie TV, Labarca C, Lester HA: Allosteric control of gating and kinetics at P2X₄ receptor channels. *J Neurosci* 1999;19:7289-7299.
- 39 Asatryan L, Popova M, Perkins D, Trudell JR, Alkana RL, Davies DL: Ivermectin antagonizes ethanol inhibition in purinergic P2₄ receptors. *J Pharmacol Exp Ther* 2010;334:720-728.
- 40 Manohar M, Hirsh MI, Chen Y, Woehrle T, Karande AA, Junger WG: ATP release and autocrine signaling through P2X₄ receptors regulate $\gamma\delta$ T cell activation. *J Leukoc Biol* 2012;92:787-794.
- 41 Gong QJ, Li YY, Xin WJ, Zang Y, Ren WJ, Wei XH, Li YY, Zhang T, Liu XG: ATP induces long-term potentiation of c-fiber-evoked field potentials in spinal dorsal horn: The roles of P2X₄ receptors and p38 MAPK in microglia. *Glia* 2009;57:583-591.
- 42 Li C, Peoples RW, Weight FF: Ethanol-induced inhibition of a neuronal P2X purinoceptor by an allosteric mechanism. *Br J Pharmacol* 1998;123:1-3.
- 43 Michel AD, Chambers LJ, Walter DS: Negative and positive allosteric modulators of the P2X₇ receptor. *Br J Pharmacol* 2008;153:737-750.